Biomaterials 33 (2012) 4031–4043

Contents lists available at SciVerse ScienceDirect

Biomaterials

journal homepage: www.elsevier.com/locate/biomaterials

# Prenatally engineered autologous amniotic fluid stem cell-based heart valves in the fetal circulation

Benedikt Weber [a], Maximilian Y. Emmert [a], Luc Behr [b], Roman Schoenauer [a], Chad Brokopp [a], Cord Drögemüller [c], Peter Modregger [d,e], Marco Stampanoni [d,f], Divya Vats [g], Markus Rudin [g], Wilfried Bürzle [h], Marc Farine [h], Edoardo Mazza [h,i], Thomas Frauenfelder [j], Andrew C. Zannettino [k], Gregor Zünd [a], Oliver Kretschmar [l], Volkmar Falk [a], Simon P. Hoerstrup [a,*]

[a] Swiss Center for Regenerative Medicine and Clinic for Cardiovascular Surgery, University Hospital Zurich, Raemistrasse 100, CH-8091 Zurich, Switzerland
[b] IMM Recherche, Institut Mutualiste Montsouris, 42 boulevard Jourdan, 75014 Paris, France
[c] Institute of Genetics, Vetsuisse Faculty, University of Berne, Bremgartenstrasse 109a, CH-3001 Berne, Switzerland
[d] Swiss Light Source, Paul Scherrer Institute, CH-5232 Villigen, Switzerland
[e] University of Lausanne, School of Biology and Medicine, Rue du Bugnon 21, CH-1015 Lausanne, Switzerland
[f] Institute for Biomedical Engineering, University and ETH Zurich, ETZ-F-85, Gloriastrasse 35, CH-8092 Zurich, Switzerland
[g] Animal Imaging Center, Institute for Biomedical Engineering, University and ETH Zurich, Gloriastrasse 35, CH-8092 Zurich, Switzerland
[h] Department of Mechanical and Process Engineering, ETH Zurich, Sonneggstrasse 3, CH-8092 Zurich, Switzerland
[i] Swiss Federal Laboratories for Materials Science and Technology, EMPA, Überlandstrasse 129, CH-8600 Dübendorf, Switzerland
[j] Department of Medical Radiology, Institute of Diagnostic Radiology, University Hospital Zurich, Raemistrasse 100, CH-8091, Switzerland
[k] Mesenchymal Stem Cell Group, Faculty of Health Sciences, University of Adelaide, PO Box 14 Rundle Mall, Adelaide, SA 5000, Australia
[l] Department of Pediatric Cardiology, University Children's Hospital Zurich, Steinwiesstrasse 75, CH-8032 Zurich, Switzerland

ARTICLE INFO

*Article history:*
Received 10 September 2011
Accepted 29 November 2011
Available online 14 March 2012

*Keywords:*
Amniotic fluid stem cells
Composite matrix
Fetal model
Heart valve
Prenatal intervention
Tissue engineering

ABSTRACT

Prenatal heart valve interventions aiming at the early and systematic correction of congenital cardiac malformations represent a promising treatment option in maternal-fetal care. However, definite fetal valve replacements require growing implants adaptive to fetal and postnatal development. The presented study investigates the fetal implantation of prenatally engineered living autologous cell-based heart valves. Autologous amniotic fluid cells (AFCs) were isolated from pregnant sheep between 122 and 128 days of gestation via transuterine sonographic sampling. Stented trileaflet heart valves were fabricated from biodegradable PGA-P4HB composite matrices ($n = 9$) and seeded with AFCs in vitro. Within the same intervention, tissue engineered heart valves (TEHVs) and unseeded controls were implanted orthotopically into the pulmonary position using an in-utero closed-heart hybrid approach. The transapical valve deployments were successful in all animals with acute survival of 77.8% of fetuses. TEHV in-vivo functionality was assessed using echocardiography as well as angiography. Fetuses were harvested up to 1 week after implantation representing a birth-relevant gestational age. TEHVs showed in vivo functionality with intact valvular integrity and absence of thrombus formation. The presented approach may serve as an experimental basis for future human prenatal cardiac interventions using fully biodegradable autologous cell-based living materials.



## 1. Introduction

Several strategies have been applied in recent years to overcome the lack of living autologous replacement materials for the repair of congenital cardiovascular malformations. Currently used artificial prostheses are associated with inherent limitations and adverse side-effects including the principal lack of growth and regeneration capacity, the increased risk of infections and the need for life-long anti-coagulation therapy [1–3]. Tissue engineering technologies may have the potential to overcome these shortcomings as indicated by a series of preclinical trials [4–7]. Particularly, the principle of pediatric heart valve tissue engineering involving the prenatal in vitro fabrication of living autologous replacement materials with growth and regeneration capacities appears promising. A prerequisite for this approach is the availability of autologous living cells prior to birth. Fetal cells, such as amniotic fluid cells (AFCs), which

* Corresponding author. Tel.: +41 44 255 3644; fax: +41 44 255 4369.
*E-mail address:* simon_philipp.hoerstrup@usz.ch (S.P. Hoerstrup).

0142-9612/$ – see front matter © 2012 Elsevier Ltd. All rights reserved.
doi:10.1016/j.biomaterials.2011.11.087

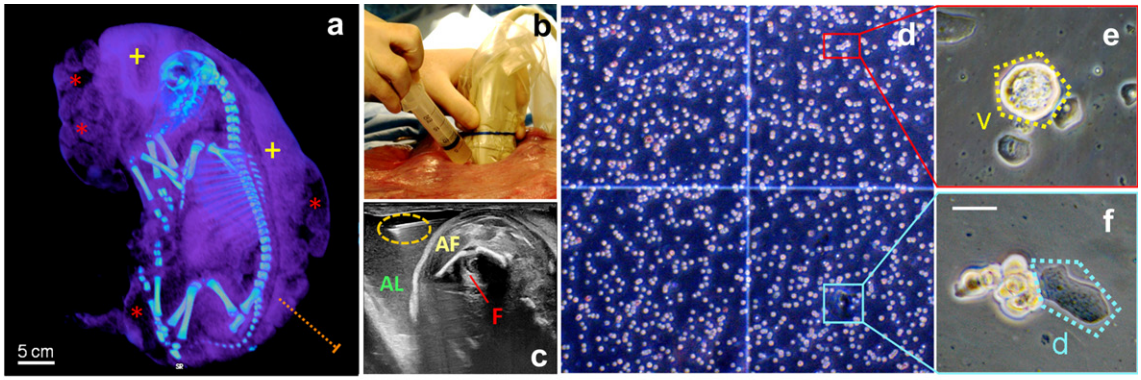
a
5 cm
b
c
AF
AL
F
d
e
V
f
d

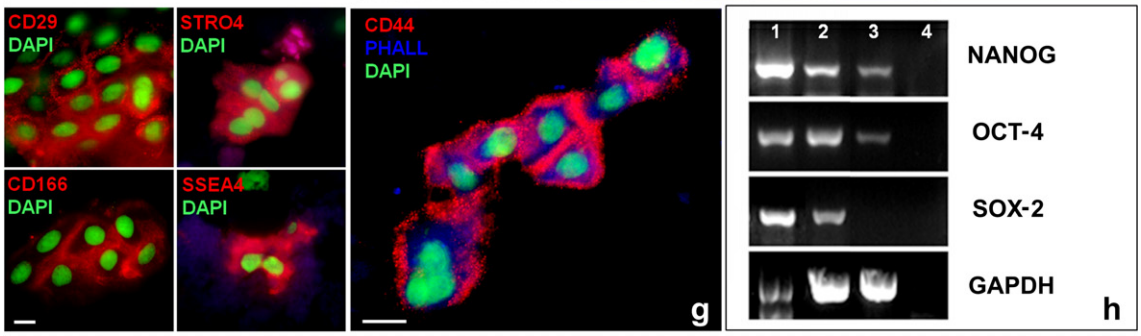
CD29
DAPI
STRO4
DAPI
CD166
DAPI
SSEA4
DAPI
CD44
PHALL
DAPI
g
1 2 3 4
NANOG
OCT-4
SOX-2
GAPDH
h

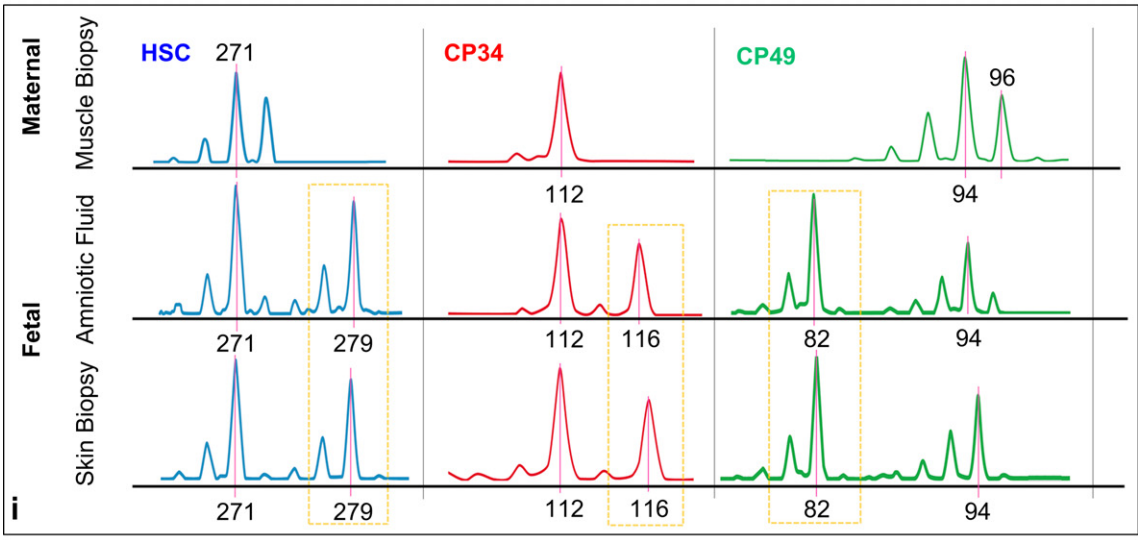
Maternal
Muscle Biopsy
HSC 271
CP34
CP49
96
Fetal
Amniotic Fluid
112
94
271 279
112 116
82 94
Skin Biopsy
271 279
112 116
82 94
i

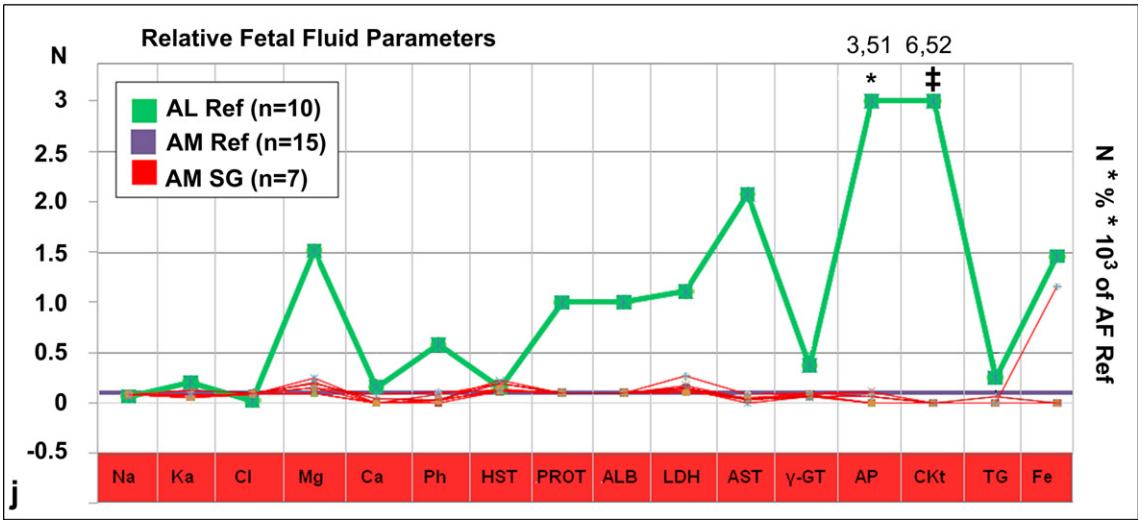
Relative Fetal Fluid Parameters
3,51 6,52
N
3
2.5
2.0
1.5
1.0
0.5
0
-0.5
AL Ref (n=10)
AM Ref (n=15)
AM SG (n=7)
N * % * 10³ of AF Ref
Na Ka Cl Mg Ca Ph HST PROT ALB LDH AST γ-GT AP CKt TG Fe
j

can be obtained already during pregnancy with minimal risk for the fetus and the mother, have been demonstrated to be appropriate for the in vitro production of heart valves [2,3,8]. After intra-uterine diagnosis of the cardiac malformation, AFCs obtained by routine amniocentesis can be used for fabrication of viable autologous constructs during pregnancy for implantation at, or shortly after birth [9]. While this concept using autologous living replacements with growth capacity addresses postnatal damage to the immature heart, intra-uterine cardiovascular damage and valve-related fetal demise cannot be prevented. The prenatal implantation of autologous cell-based growth-adaptive tissue engineered heart valves would allow for an even earlier repair of the defect potentially avoiding secondary cardiovascular maldevelopment and preventing fetal demise. In addition, the favorable fetal regeneration environment involving enhanced, scarless healing [10], capacity of myocyte proliferation [11] or high blood levels of progenitor cells [12] may promote optimal remodeling of the implanted constructs.

The principal feasibility of fetal cardiac interventions has been proven both, in selected human fetuses [13], and experimental animal models involving fetoscopic, trans-umbilical and catheter-based approaches [14,15]. Clinically, successful fetal cardiac catheterization and balloon valvuloplasty by direct puncture of the obstructed valve segment have been shown by several groups [13,16–21]. Although encouraging, valvular re-stenosis of the obstructed portions has repeatedly been reported after prenatal cardiac balloon interventions [17,21]. The implantation of fully biodegradable tissue engineered heart valves (TEHVs) into the orthotopic valve position would improve the sustainability of the valvular repair by dilating the obstructive segment, restoring normal valve functionality as well as preventing re-stenosis. The presented study investigates the prenatal minimally invasive implantation of autologous amniotic fluid stem cell-based tissue engineered heart valves in the ovine fetal model using an in-utero closed-heart hybrid single-step intervention technique.

## 2. Methods

### 2.1. Scaffold fabrication

Trileaflet heart valve scaffolds ($n = 9$) were fabricated from non-woven polyglycolic-acid meshes (PGA; Cellon, Luxembourg) and coated with 1.75% poly-4-hydroxybutyrate (P4HB; TEPHA Inc., USA) by dipping into a tetrahydrofuran solution (Fluka, Germany). Thereafter, the scaffolds were integrated into radially self-expandable nitinol stents (OptiMed, Germany, OD 10.0–12.0 mm) by attaching the scaffold matrix to the inner surface of the stent wires using single interrupted sutures (Ethicon, USA; Suppl. Methods A).

### 2.2. Amniotic fluid cells

#### 2.2.1. Isolation and seeding of AFCs

After transuterine puncture, amniotic fluid was aspirated into a 50 mL syringe using a 10 Gauge needle under sonographic guidance (Philips, Medical Systems, The Netherlands). Amniotic fluid cells (AFCs) were obtained by centrifuging the fluid at 280 G for 10 min and removing the supernatant. The viability of isolated AFCs was determined using trypan blue exclusion staining (Sigma Chemical Co., USA) and hemocytometry. TEHVs were prepared for cell-seeded and unseeded (fibrin-coated) control valve implantations ($n = 9$). Seeding of autologous AFCs onto the stented heart valve scaffolds ($5.0 \pm 3.8 \times 10^6$ cells/cm$^2$) was performed using fibrin as a cell carrier according to a standardized protocol [22]. After a short incubation period, the seeded constructs were loaded into the delivery system (14 F, Cook Medical Inc., USA) by decreasing the outer diameter from 10.0/12.0 mm to 4.7 mm (Suppl. Methods B).

#### 2.2.2. Genotyping of cells

5 mL of ovine amniotic fluid was used for analysis of eleven microsatellite markers located on different sheep chromosomes (BM6444, CP34, CP49, CSRD247, FCB304, HEL13, HSC, HUJ616, ILSTS30, INRA63, JMP29). The results were compared to fetal as well as maternal muscle and skin biopsies (Suppl. Methods C).

#### 2.2.3. Differential fetal fluid analysis

For exclusion of allantoic fluid aspiration, 1 mL of supernatant ($n = 7$) was collected and values of amniotic fluid-specific parameters, including Na (sodium), K (potassium), Cl (chlorine), Mg (magnesium), Ca (calcium), Ph (phosphate), urea, protein, albumin, lactate dehydrogenase, γ-glutamyl-transferase, aspartate aminotransferase, alkaline phophatase, creatin kinase, triazylglycerine, and Fe (iron) were determined using either photometric or colorimetric protocols (Cobas®, Roche Diagnostics, Switzerland; Suppl. Methods D) and compared to amniotic ($n = 15$) as well as allantoic ($n = 10$) fluid reference samples.

#### 2.2.4. Phenotyping of AFCs

Small samples of isolated AFCs were analyzed using immunohistochemistry and semiquantitative RT-PCR analysis. Primary antibodies used for characterization were against CD29 (anti-ovine CD29; A. Zannetino), Stro4 (anti-ovine STRO-4, A. Zannetino), CD44 (sc-59758, Santa Cruz, Inc., USA, Clone NKI-P2), CD166 (5E10; Clone 3A6), and SSEA-4 (clone MC-813-70, DSHB). Primary antibodies were detected with Cy-2 or Cy-3 goat-anti-mouse and Cy-5 goat-anti-rabbit secondary antibodies (Jackson Immunoresearch Inc., USA). To verify expression of pluripotency genes, RT-PCR analysis for NANOG, SOX-2 and OCT-4 was performed (Suppl. Methods E).

#### 2.2.5. Transwell migration assay

Isolated ovine AFCs (oAFCs) were seeded onto PGA-P4HB scaffold matrices or directly plated into the lower chamber of transwell culture plates (BD Falcon). Migration of peripheral blood-derived mononuclear cells was carried out for 300 min at 37 °C, 5% $CO_2$ and the number of migrated cells was determined using hemocytometry with comparison to negative control migration (Suppl Methods F).

#### 2.2.6. Cytokine profiling

For exemplary analysis of cytokine secretion by AFCs in vitro, isolated cells were incubated in growth factor-depleted EGM™-2 medium (Lonza Group AG, Switzerland; hAFCs [2009-0095]). After 2 days the supernatant was collected and analyzed using the Proteome Profiler Array Kit (ARY005; R&D Systems, Inc., USA) according to the manufacturer's instructions (Suppl Methods G).

### 2.3. Planar fluorescence reflectance imaging (pFRI)

For analysis of cellular loss during valvular crimping the seeded constructs were placed into the MAESTRO™ imaging system (Maestro 500; Cambridge Research Inc., USA). For detection of CFSE-labeled amniotic fluid cells pre- and post-crimping (CellTrace™; CFSE Cell Proliferation Kit; C34554, Invitrogen Corp., USA) a band pass filter from 445 nm to 490 nm was used. The signal from the CFSE-labeled AFCs pre- and post-crimping (crimping time: 10 min) was compared after normalization and quantified (Suppl. Methods H).

### 2.4. Animal welfare and anesthetic protocol

Nine pregnant Pre-Alp sheep between 122 and 128 days' gestation were used for the study (term 143 days, fetal mean weight ~1500 g). All animals received humane care in compliance with the "Principles of Laboratory Animal Care" (NIH publication no.85–23, revised 1985). All procedures were approved by the Institutional Ethics Committee [10-16QRF30A]. In case of twins only one fetus was subjected to TEHV implantation, to avoid collateral bias. After overnight fasting, each animal was sedated by intravenous injection of pentothal (10 mg/kg body weight). Sheep were placed into a supine position, intubated, ventilated with 100% oxygen and 1–2% isoflurane (Suppl. Methods I).

**Fig. 1.** Isolation of autologous amniotic fluid cells. Amniotic fluid (AF, a:+) was aspirated via a transuterine puncture under songraphic guidance (a–c; needle = yellow circle) carefully avoiding laceration of the fetus (F) as well as aspiration of allantoic fluid (AL, a:*). Isolated amniotic fluid cells (AFCs) were analyzed using trypan blue exclusion staining (d; SB ~ 20 μm) revealing cell viability with high variability (31–69%). Isolated non-adherent cells showed different morphologies (e–f; v = vesicular/bright; d = dark/flattened; bright field) and stained positively for several stem cell markers including CD29, STRO-4, CD166, SSEA-4, and CD44 (g; SB ~ 15 μm). Specific staining is shown in red, DAPI (nuclei in green) and Phalloidin (*f*-actin in blue) were used as control stainings. In RT-PCR analysis (h) AFCs (1) showed expression of several stem cell factors on the mRNA-level involving NANOG, OCT-4, and SOX-2 compared to ovine bone marrow-derived MSCs (2), ovine myofibroblasts (3) and negative controls (4; GAPDH served as house-keeping control gene). Autologous fetal origin was confirmed using microsatellite analysis, comparing fetal amniotic fluid and skin biopsies to the maternal signal (i). Amniotic fluid nature of study samples was analyzed by comparing electrolyte and enzyme parameters (j) to amniotic fluid (AM) and allantoic fluid (AL) reference samples. Parameters were normalized to amniotic fluid (violet curve: $0.1 \times 10^3$%) showing close correlation of study samples (red curves) with amniotic fluid reference material, and missing correlation with allantoic fluid reference material (green curve; $R = 0 - 6.5 \times 10^3$%; extrema indicated by */‡ are given in absolute numbers). (For interpretation of the references to colour in this figure legend, the reader is referred to the web version of this article.)

### 2.5. TEHV implantation

After sonographic assessment (Philips Healthcare iE33®xMATRIX-Ultrasound System; The Netherlands), the uterus was exteriorized through a maternal midline laparotomy and the fetal heart was approached via two different routes: a) the fetus was left in-utero and, following trans-uterine thoracotomy, its skin was sutured to the uterine wall, or b) after partial externalization from the uterus, thoracotomy was performed. The fetal chest was opened via left-sided mini-thoracotomy at the 4th intercostal space. Following pericardiotomy, a 5/0 pledged purse-string suture was placed on the right antero-apical region of the fetal heart (TI-CRON®-5-0, Syneture Suture, IPP Pharma, France). Thereafter, a 16 Gauge catheter was inserted into the apex of the right ventricle and a guide-wire was introduced into the catheter and through the ductus arteriosus into the descending aorta. A 14 French delivery system (Zenith-Flex®, Cook Medical, USA) was then mounted onto the guide-wire and advanced to the landing zone of the orthotopic pulmonary valve position. After deployment, the position of the TEHVs was confirmed using echocardiography and angiography, the implantation-site was closed using pre-placed 5/0-pledged purse-string sutures and fetal fluids were re-infused into the uterus. The fetuses were harvested postoperatively (acute), at midterm (300 min after delivery), as well as at long-term (depending on survival up to 1 week after implantation, BRGA = birth relevant gestational age). At harvest, echocardiography and contrast angiography were performed, and TEHV position was assessed at necropsy (Suppl. Methods J-K).

### 2.6. Qualitative explant tissue analysis

Explanted TEHV constructs ($n = 9$) were evaluated macroscopically. Their tissue composition was analyzed qualitatively by histology and compared to native heart valve leaflets. The tissue sections were studied using von Kossa, H&E, Masson-Trichrome, and eVG staining. In addition, immunohistochemistry was performed using the Ventana Benchmark automated staining system (Ventana Medical Systems, USA) with antibodies for α-SMA (clone 1A4; Sigma Co., USA), Desmin (clone M0760; Dako), and vWF (clone A0082, Dako). Primary antibodies were detected with the Ventana *iVIEW* Diaminobenzidine detection kit (Suppl. Methods P). In addition, representative tissue samples were fixed using 2% glutaralaldehyde. After preparation, samples were sputter-coated with platin and investigated with a Zeiss Supra-50-VP-Microscope (Carl Zeiss Imaging, Germany; Suppl. Methods L).

### 2.7. Grating interferometry

AFC-seeded constructs and explanted valvular leafets (BRGA, $n = 2$) were evaluated using grating interferometry performed at the TOmographic Microscopy and Coherent rAdiology experimenTs (TOMCAT) beamline of the Swiss Light Source (SLS, Villigen, Switzerland). The samples were embedded in 2%-agarose gel and a tomographic scan was performed at a photon energy of 25 keV. The multi-slice information was combined in three-dimensional images and different stages were compared (Suppl. Methods M).

### 2.8. Cell labeling and tracking

In order to evaluate the in vivo fate of seeded AFCs, cells were tracked up to 1 week in vivo using the CellTrace™ CFSE Cell Proliferation Kit (C34554, Invitrogen Corp., USA) and/or Carboxy SNARF®-1 (carboxylic acid, acetate, succinimidyl ester/SNARF-1; C-1270, Invitrogen Corp., USA). For this purpose the pellet of the isolated AFCs was labeled according to the manufacturer's instructions prior to seeding onto the scaffold. After explantation the constructs were analyzed using confocal microscopy (Leica Microsystems, Germany; Suppl. Methods N).

### 2.9. Quantitative explant tissue analysis

Explanted TEHV leaflets were lyophilized and analyzed by biochemical assays for total hydroxyproline content and GAG content using standardized protocols [6] (see Suppl. Methods O). The cellularity of explanted TEHVs was determined by quantification of nuclei in histology (not corrected for pre-seeded AFCs).

### 2.10. Biomechanical testing

The mechanical properties of the TEHV conduits were determined by uniaxial tensile testings using a translation stage (PI-M-505-4PD, PI GmbH, Germany) and a 10 N-load-cell (force transducer KAW-S, AST, Germany). For analysis of the biomechanical properties of the TEHV leaflet (BRGA explants) nano-indentation tests have been conducted in dried conditions to determine the Modulus of Elasticity (ME; Suppl. Methods P).

### 2.11. Statistical analysis

Quantitative data are presented as mean ± standard deviation. For statistical comparison an analysis of variance (ANOVA) was performed. A $P < 0.05$ was considered statistically significant and significance levels were corrected using the post hoc *Bonferroni* method (SPSS Inc., Chicago, IL, USA).

## 3. Results

### 3.1. Prenatal isolation of amniotic fluid: An autologous fetal cell source for therapy

For fabrication of TEHVs, amniotic fluid was collected via a transuterine puncture under sonographic guidance (Fig. 1a–c; $n = 7$). On average 85.6 ± 7.2 mL of amniotic fluid could be aspirated per fetus. The puncture of the amniotic cavity (Fig. 1a–c) and the fluid aspiration was successful in all animals and neither aspiration of blood nor any fetal or maternal hemorrhage was observed. After centrifugation, 19.9 ± 15.2 × $10^6$ cells (2.38 ± 1.7 × $10^5$ per mL) were isolated from the aspirates, indicating individual disparities in cellular density. Viability was determined by trypan blue exclusion staining (Fig. 1d) and revealed high variability between different study samples (31–69%).

For evaluation of the stem cell nature of ovine AFCs, antigen expression as well as expression of stem cell factors was assessed. Isolated AFCs showed expression of the common ovine MSC-markers CD29, STRO-4, CD166, CD44, and SSEA4 (Fig. 1g) as well as mRNA expression of stem cell factors including NANOG, OCT-4, and SOX-2 comparable to ovine mesenchymal stem cell control populations (Fig. 1h). PCR microsatellite analysis revealed autologous fetal origin of aspirated AFCs (Fig. 1i). In one fetus a slight background signal could be detected suggesting minor fluid contamination by its' sibling. No maternal contamination could be observed in the fetal fluid samples.

### 3.2. Differential analysis of amniotic fluid: the exclusion of allantoic fluid contamination

Although representing the standard model for fetal interventions, the ovine pregnancy contains an allantoic fluid compartment (Fig. 1a) not present in human pregnancies at term. Therefore, analysis for amniotic fluid nature of the aspirated samples was performed. Correlation of the profile of fetal fluid electrolyte and enzyme parameters compared to values of fetal fluid reference material ($n = 25$; Fig. 1j) confirmed amniotic fluid nature of the study samples ($n = 7$) and excluded significant contamination by allantoic fluid aspiration.

### 3.3. Amniotic fluid cell-based TEHVs: viable autologous constructs for prenatal minimally invasive implantation

After isolation, AFCs were seeded onto PGA-P4HB composite heart valve scaffolds (4.0 ± 3.1 × $10^6$ cells/$cm^2$; Fig. 2a–b) using fibrin as a cell carrier. As shown with grating interferometry (GI; Fig. 2c–d) the fibrin matrix containing AFCs was equally distributed over the full thickness of the scaffold matrix. The seeded constructs were crimped and loaded into the application device (Fig. 2e–h). Unseeded controls were coated with fibrin only and treated accordingly. The overall crimping time from insertion to valvular deployment was 5.6 ± 2.8 min, and no re-crimping was necessary. As evaluated in vitro by pFRI analysis (Fig. 2i–l) of valves seeded with CSFE-labeled AFCs maximum crimping did not result in a substantial loss of cells (Fig. 2l).

### 3.4. Fetal transapical valve implantation: an in-utero closed-heart hybrid technique

After mounting onto the guide wire, the delivery system was introduced into the ventricle via an antero-apical incision (Fig. 3a)

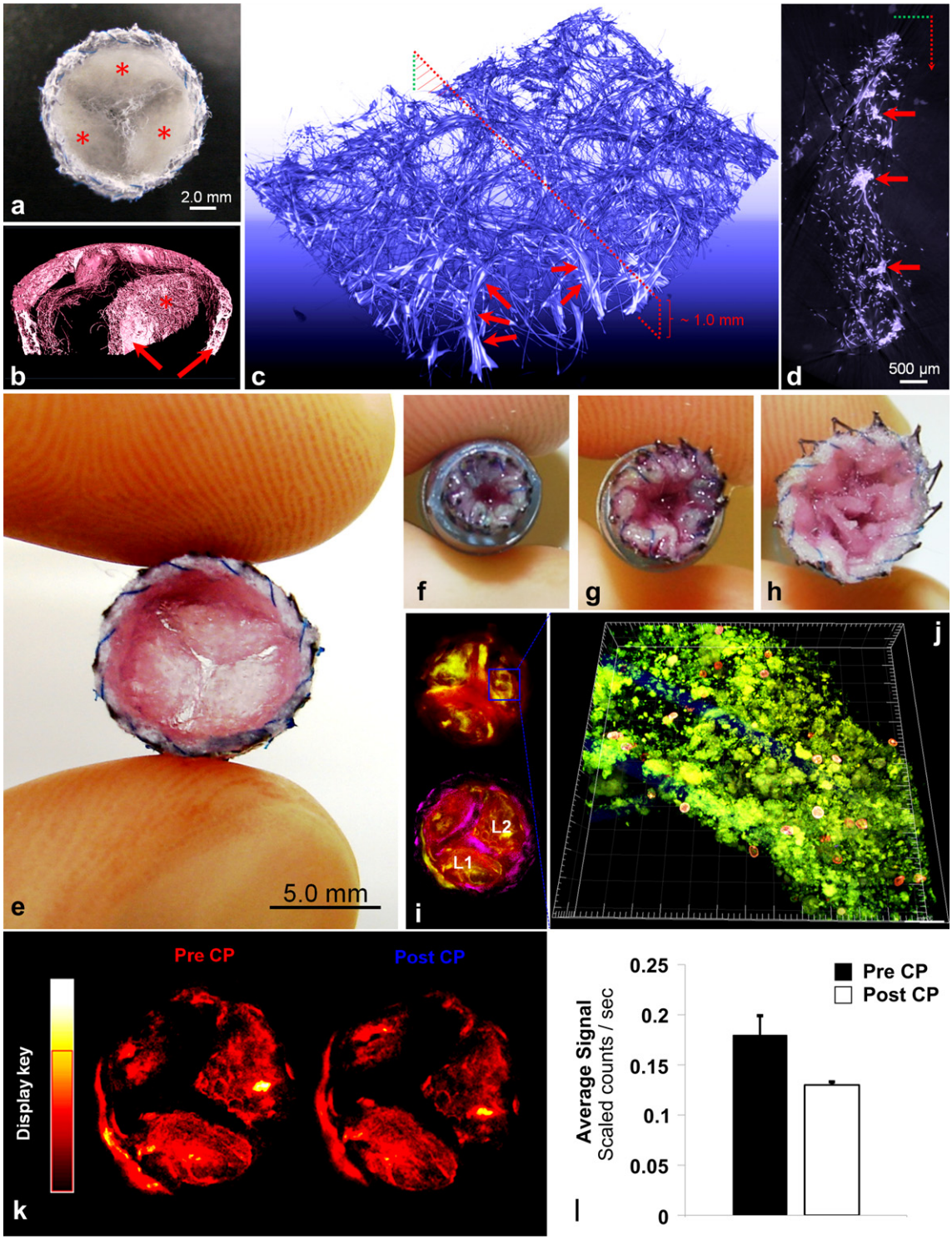


**Fig. 2.** Fabrication of amniotic fluid cell-based heart valves in vitro. PGA-based valve shaped matrices were integrated into self-expandable nitinol stents (a; * = leaflets) and coated with P4HB as indicated in the micro-CT analysis (b, arrows = PGA-P4HB-composite matrix). Grating interferometry demonstrated equal distribution of the fibrin matrix containing AFCs over the composite scaffold matrix (c-d; arrows indicate fibrin matrix) of TEHVs (e). After seeding of AFCs, TEHVs (e) were crimped and introduced into the delivery system (f–h). For analysis of cellular loss during the crimping procedure in vitro, AFCs were labeled with CFSE and seeded onto trileaflet starter matrices as visualized with pFRI (i; red = autofluorescence and yellow = specific signal) and with confocal microscopy (j; green = CFSE labeled AFCs). Before crimping (k; PreCP) the average fluorescence signal of two representative areas (i, L1-2) was determined and compared to the signal after a ~10 min crimping phase (k, PostCP) showing loss of 27.8% of average signal after maximum crimping (l; scaled counts/sec ± SD). (For interpretation of the references to colour in this figure legend, the reader is referred to the web version of this article.)

and advanced to the defined landing zone of the orthotopic pulmonary valve position (Fig. 3b–d). The deployment of the TEHVs was successful in all animals ($n = 9$) and proper opening and closing behavior of the TEHVs could be demonstrated by angiography (Fig. 3e–i; Video 1) and transepicardial echocardiographic measurements (Fig. 3j–n; Video 2-3). However, the introduction of the delivery device into the right ventricle was challenging in all fetuses and major blood loss occurred in two of

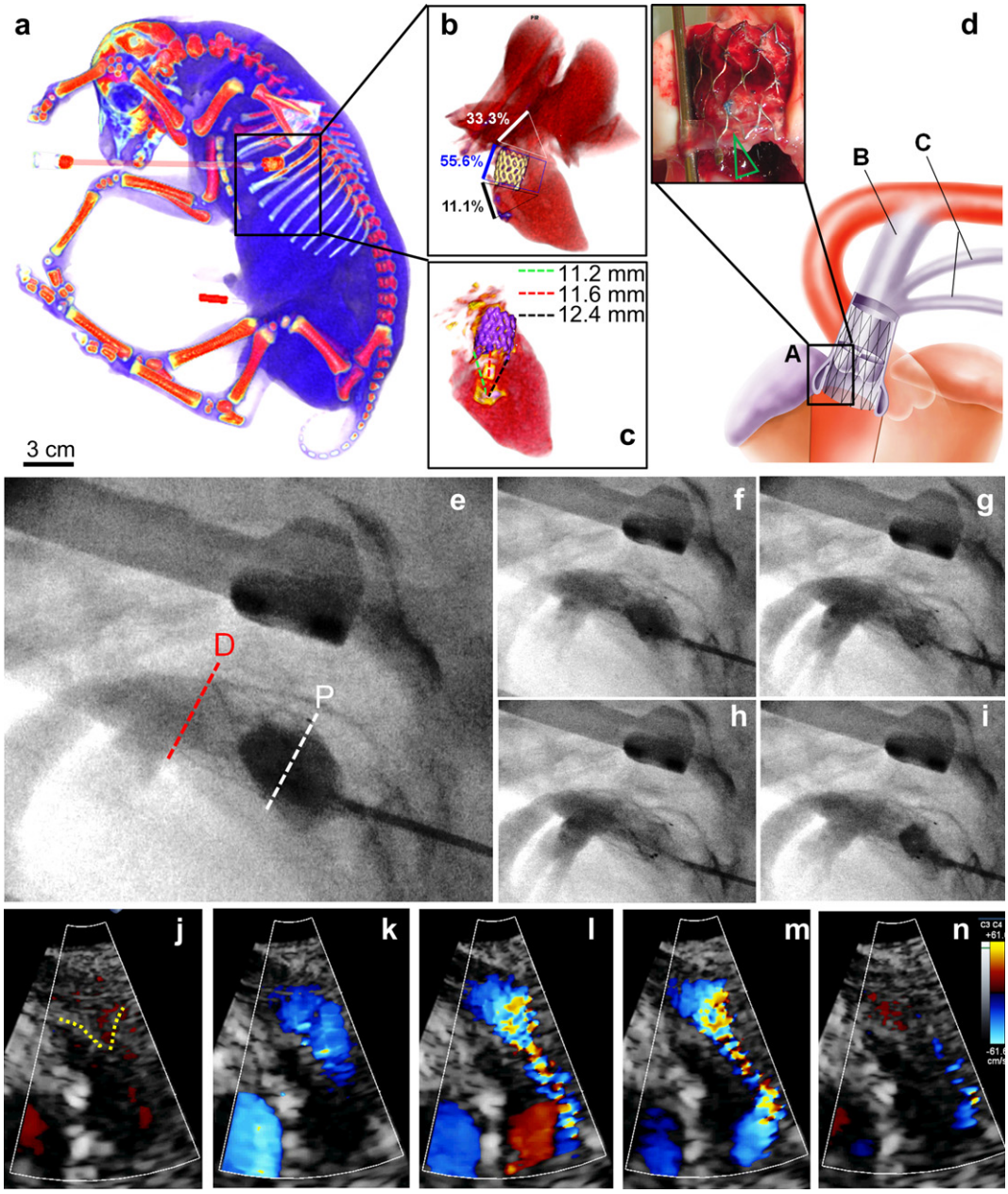


**Fig. 3.** Transapical fetal implantation of tissue engineered heart valves. For implantation of the TEHVs, the fetal chest was opened at the 4th intercostal space (a) and the device was inserted into the fetal heart (a–d). The device was advanced 11.7 ± 0.6 cm to the defined landing zone of the orthotopic pulmonary position (c, d(A); c = mean distance from the ventricle entry point to the proximal stent margin) proximal to the DA Botalli (d, B) and the pulmonary arteries (d, C). In 33.3% of implants TEHV deployment was distal to the annulus (b) and required surgical exclusion of valvular leaflets. In the remaining implants the stented TEHVs excluded the native valve leaflets (b; d: green arrow = native leaflet). Post-deployment angiography revealed adequate perfusion of adjacent great arteries (e–i; D = distal; P = proximal stent ending) and echocardiography showed leaflet mobility and functionality (j–n; Color Doppler mode). (For interpretation of the references to colour in this figure legend, the reader is referred to the web version of this article.)

the animals, which did not survive the acute postoperative phase. No fetal cardiac bypass or blood substitution was used. In 66% of all implants the stent was successfully deployed into the pre-defined landing zone of the orthoptopic pulmonary valve position, while in 33% the positioning of TEHVs was supravalvular necessitating exclusion of single native leaflets to enable TEHV loading during diastole for proper functionality (Fig. 3b–d). The mean procedure duration from harvest to delivery was 86 ± 26 min. In all fetuses contrast angiography as well as trans-epicardial echocardiography displayed normal perfusion of the pulmonary vasculature and the Ductus Botalli (Fig. 3e–n). No migration or paravalvular leakage was observed.

Supplementary data related to this article can be found online at doi:10.1016/j.biomaterials.2011.11.087.

### 3.5. *In vivo performance of TEHVs: valve function of prenatally engineered constructs until birth*

TEHVs were explanted after the acute implantation (30 min; $n = 3$), 300 min after delivery (midterm explants; $n = 2$) or left in utero for long term assessment ($n = 4$). Acutely harvested valves showed intact and mobile leaflet structures (Fig. 4a). Fluoroscopy and echocardiography indicated adequate valvular functionality and presence of leaflet co-aptation (Fig. 4d,g). Also midterm TEHV

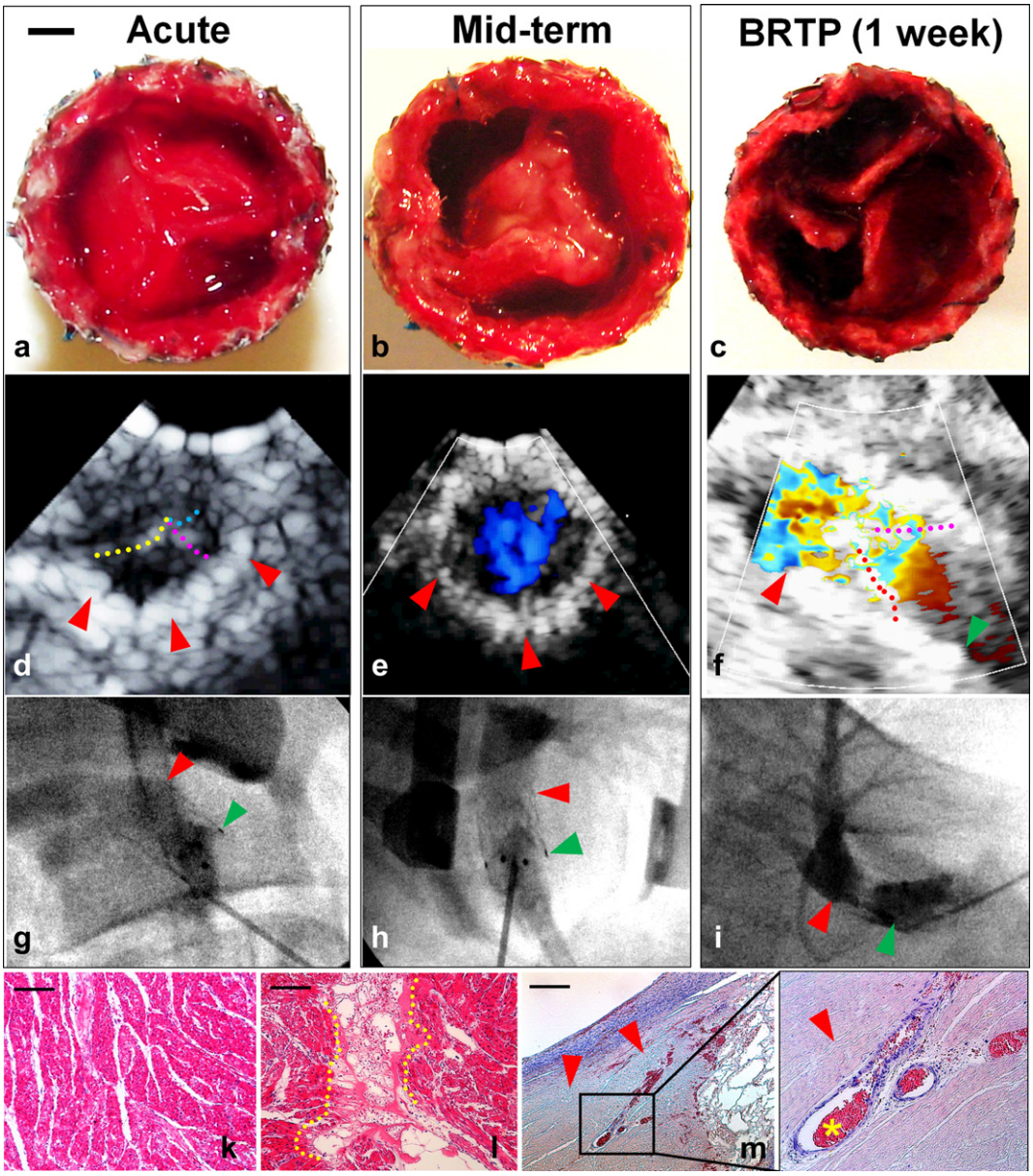


**Fig. 4.** In-vivo functionality and explant morphology. Macroscopic, echocardiographic and angiographic pictures of acute (a,d,g), mid-term (b,e,h) and long term (c,f,i; BRTP) explants (arrows indicate proximal and distal stent endings). In chronic (BRTP) explants of the scar region substantial remodeling in the necrotic region (arrows; k-m; SB ~ 400 μm) with in-growth of large caliber vessels (m; arrows) could be observed, when compared to healthy fetal myocardium (k) and the scar region of mid-term explants (l).

leaflets showed mobile and co-adaptive leaflets with lack of regurgitation at explantation (Fig. 4e,h). However, after harvest, midterm TEHV explants presented with thickened leaflets as well as conduit areas (Fig. 4b). No thrombus formation or impairment of valve integrity was observed. Remaining fetuses ($n = 4$) were left in-utero for evaluation of long term functionality and possible survival until birth. One fetus survived until reaching a birth relevant gestational age (BRGA) of ~ 133 days, whereas the remaining fetuses presented with premature demise (2–5 days post implant). At BRGA leaflet mobility and valvular functionality could be demonstrated using echocardiography and angiography (Fig. 4f,i). TEHV leaflets explanted at BRGA showed leaflet integrity and absence of thrombus formation; however, one leaflet clearly showed radial shortening of about 1/3 of the radial leaflet extension (Fig. 4c). Histological analysis of the antero-apical ventricular scar region revealed substantial remodeling with large-caliber vascular in-growth (Fig. 4k–m).

### *3.6. Histological analysis of explanted constructs - the stages of remodeling*

Explanted TEHVs as well as native fetal pulmonary valve control samples were harvested and investigated histologically (Fig. 5a–t). Acute TEHV explants (Fig. 5e–h) were mainly composed of an intact fibrin carrier matrix and initial cellular infiltration. After mid-term in-vivo function, explanted cell-seeded TEHVs showed enhanced localized phagocytic infiltrations of the constructs (Fig. 5i–l). SEM confirmed cellular presence also on the surface of the explants (Fig. 5u–v). Histology of BRGA explants (Fig. 5m–t) showed clear tissue formation indicated by collagen-rich, α-SMA-positive regions in the conduit as well as in the leaflet hinge area (Fig. 5o–p), without a confluent endothelial cell layer on top (Suppl. Fig. 1). In addition, a profound primary phagocytic infiltration was observed. A core scaffold remnant was

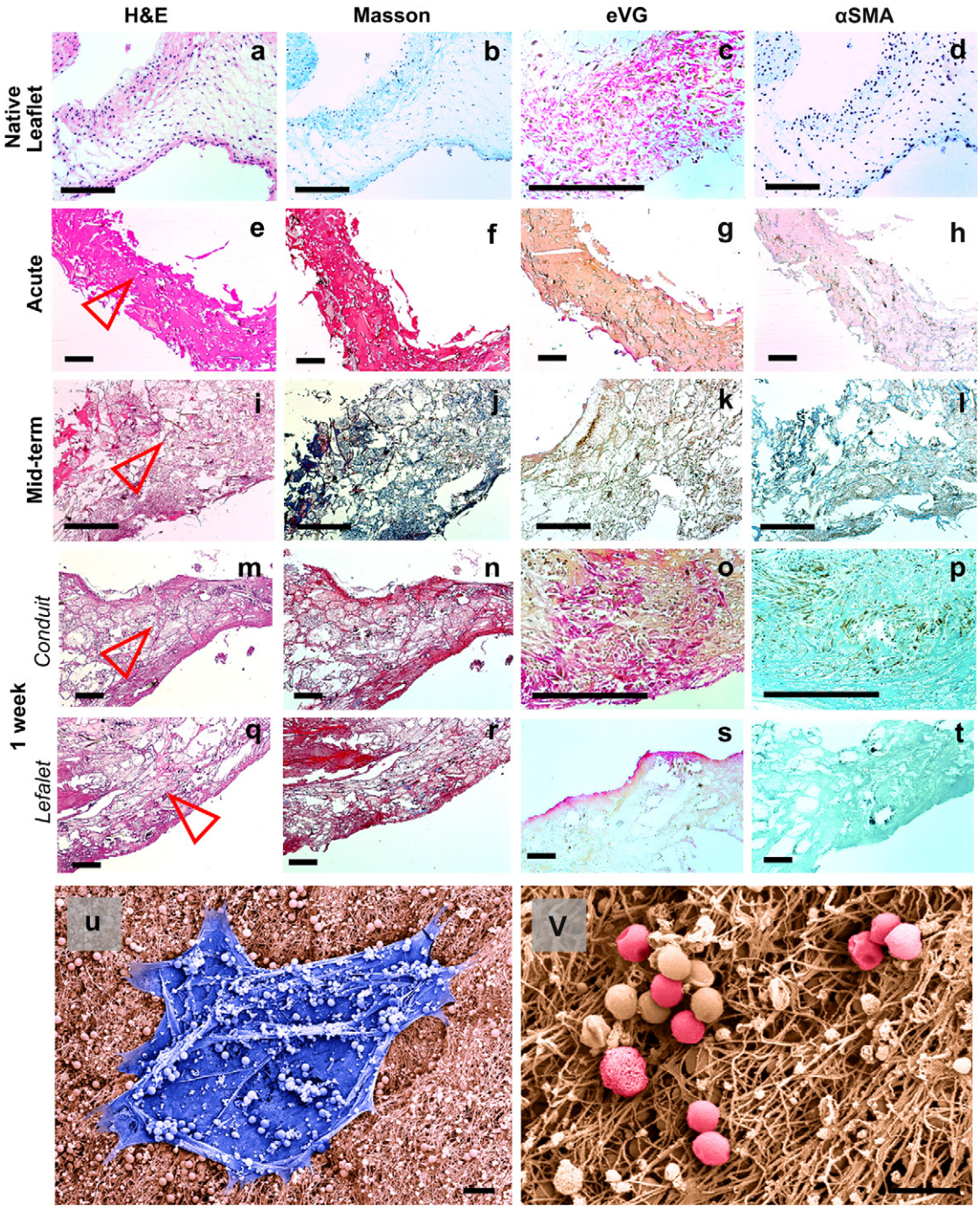


**Fig. 5.** Histology of explanted tissues. Comparative histology of native leaflets (a–d), acute explants (e–h), mid-term explants (i–l), and long term (BRGA) explants (m–t). H&E-staining shows the decrease of originally seeded fibrin matrix with the time in vivo. Masson and eVG stainings demonstrate initial collagen formation in the long term explants (o, s) with lack of collagen at earlier stages. Presence of α-SMA positive cells was also only detectable in the late explants stages (p). A central scaffold core was visible in all explants (red arrows; e,i,m,q; SB ~ 250 μm). In midterm explants SEM analysis revealed initial fibrin deposition (u) combined with cells visible on the surface (v; SB ~ 20 μm). (For interpretation of the references to colour in this figure legend, the reader is referred to the web version of this article.)

found in the center of the explanted TEHVs and constituents of the composite matrix could be identified in all explant stages (Fig. 5a–t, red arrows).

### 3.7. Qualitative analysis of explants - cellularity and cell tracking

Explanted TEHVs were analyzed using cellularity quantification and extracellular matrix (ECM) analysis for HYP (hydroxyproline) and GAG (gylcosaminoglycan) levels. The cellularity of the pre-seeded TEHV constructs increased significantly after 300 min and/or 1 week after implantation (all P's $< 0.05$; Fig. 6a). Also comparison of the cellularity between cell-seeded versus unseeded controls of acute or mid-term explants revealed higher cellularity of pre-seeded TEHVs versus unseeded constructs (Fig. 6a–b; not controlled for pre-seeded AFCs). Cellularity was highest in BRGA explants; however, none of the animals with unseeded constructs could be followed until BRGA for comparison of cellularity at this time point. In addition, ECM analysis

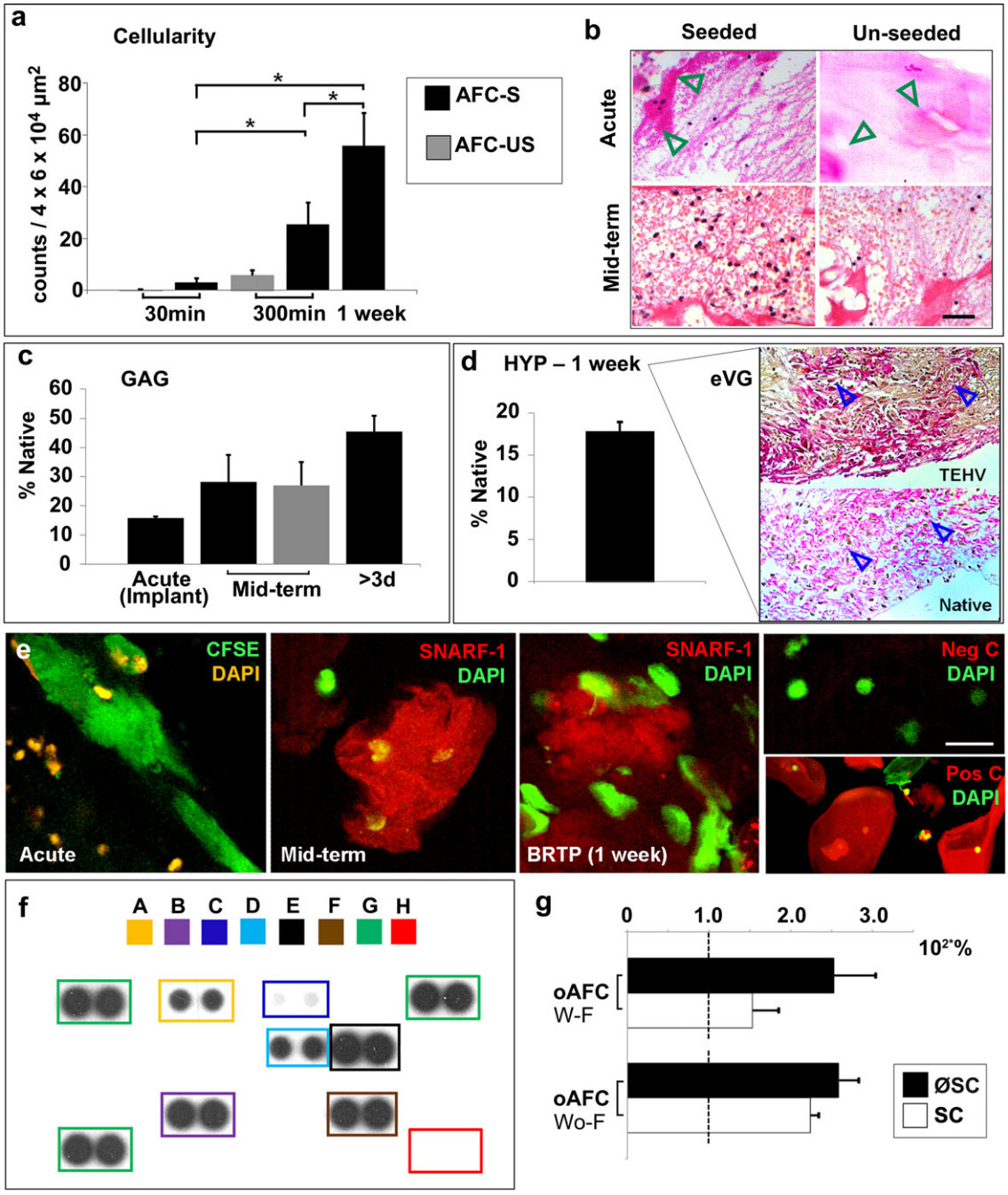


**Fig. 6.** Cellularity and chemo-attractive potential. Analysis of the cellularity and extracellular matrix revealed significantly increasing cellularity (*$P < 0.05$) and increasing GAG-values in the TEHVs with increasing time in-vivo (a-c; b: SB ~ 75 µm). Acutely as well as at mid-term un-seeded control leaflets presented with lower cellularity in explanted TEHV tissues (a–b; not corrected for pre-seeded AFCs), while GAG values were comparable. Already after 1 week in vivo initial formation of collagen (HYP) was detectable biochemically as well as on the structural level in eVG-stainings (d; TEHV). CFSE/SNARF-1 labeled AFCs were detectable directly after implantation (acute), after several hours (midterm) as well as 1 week after implantation, but with decreasing numbers (e; SB ~ 10 µm). In vitro, AFCs secrete various cytokines as measured with a standard proteome profiler array (f; hAFCs; A = CXCL-1, B = MIF, C = sICAM-1, D = IL-6, E = IL-8/CXCL-8, F = Serpin-E-1, G = positive control, H = negative control). In cell-migration-analyses isolated ovine AFCs and pre-seeded AFC-based matrices show higher migration of mononuclear cells in comparison to negative controls (g; relative to negative control migration = black line). [AFC-S = AFC-seeded; AFC-US = AFC-unseeded; ØSC/SC = Without/With PGAP4HB-scaffold].

revealed that the constructs' GAG contents increased during in vivo conditioning, reaching maximum levels 1 week after implantation (Fig. 6c) indicating ECM remodeling. The collagen content in the explanted tissue samples after 1 week in vivo was substantially lower in the newly formed tissues than compared to native fetal controls (Fig. 6d). For evaluation of the presence of seeded AFCs, cell-tracking analysis using CFSE and/or SNARF-1 labeling agents was performed ($n = 4$). Confocal microscopy of explanted tissues clearly showed presence of seeded AFCs acutely as well as several hours after delivery. 1 week after implantation only single labeled cells could be identified suggesting replacement of primary seeded AFCs (Fig. 6e).

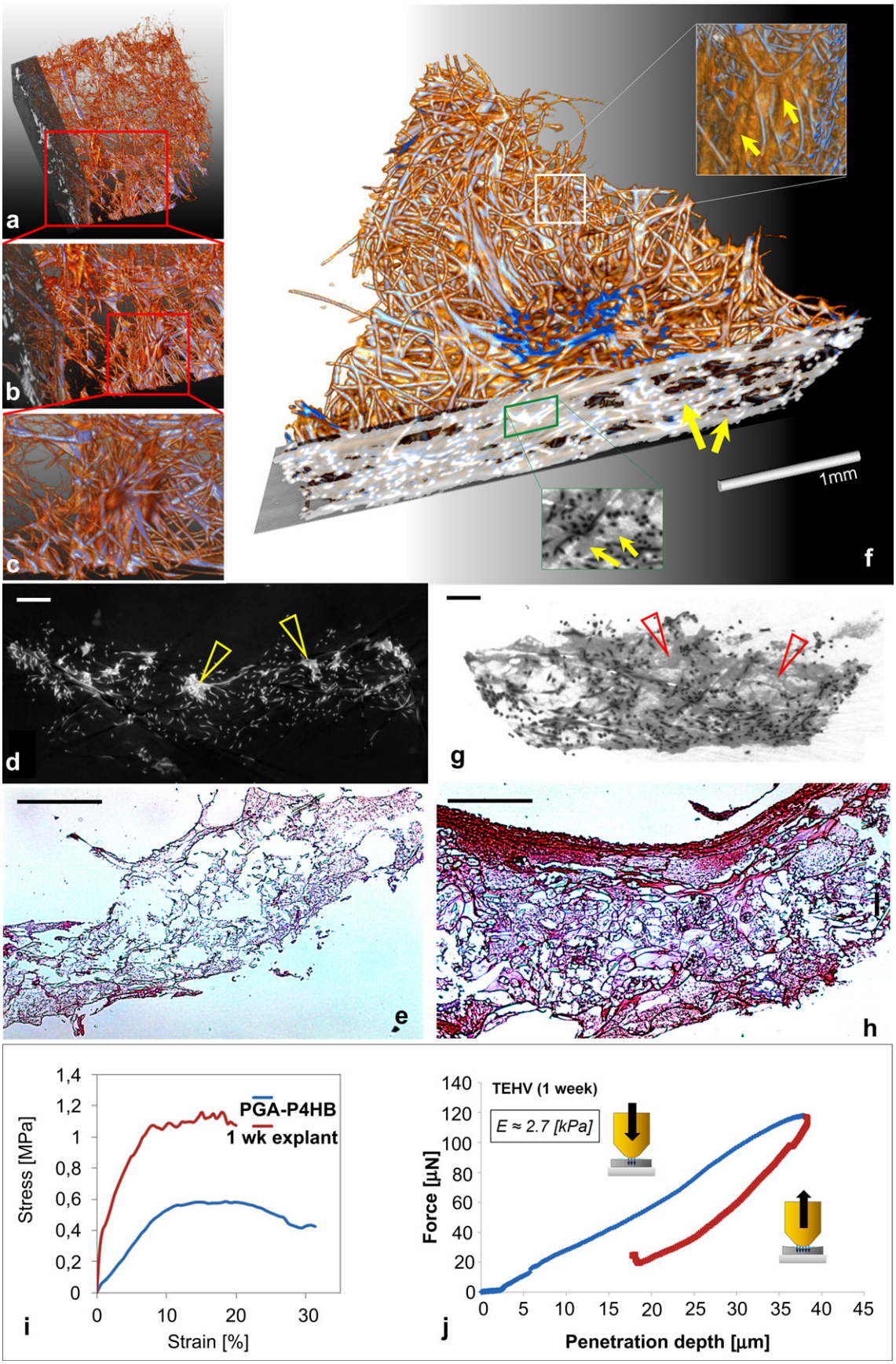


**Fig. 7.** Grating interferometry and biomechanical analysis of explants. After in vivo remodeling of seeded constructs (a–e; d: SB ~ 250 µm, yellow arrows indicate fibrin matrix; e: SB ~ 500 µm), grating interferometry of explanted TEHVs (f-h; BRGA) shows the network of the PGA-P4HB composite scaffold with tissue formation between the scaffold

### 3.8. Chemo-attractive potential and cytokine-profile of AFCs

The chemo-attractive, migratory capacity of scaffold-seeded ovine AFCs on autologous peripheral blood-derived mononuclear cells was assessed exemplarily in vitro using a cell migration assay. Compared to unseeded controls, migration was higher in the AFC-seeded constructs; however, independent of the seeding technique (Fig. 6g). To also exemplify the chemo-attractive cytokine expression of PGA-P4HB-seeded AFCs a proteome profiler array (PPA) of the culture medium of hAFCs was performed. The PPA analysis revealed release of several potential pro-angiogenic/immunomodulatory cytokines after 48h of in vitro culture including factors like CXCL-1, MIF or IL-6 (Fig. 6f).

### 3.9. Quantitative explant analysis - from scaffold to viable tissue

Long term (BRGA) explant tissues were analyzed using grating interferometry (GI) and biomechanical testing. GI microstructural 3D-tomographic analysis revealed significant tissue formation in the explanted leaflet tissues (Fig. 7a–c,f; Video 4-5). As confirmed by histology, constituents of the composite scaffold matrix (PGA-P4HB) could be identified (Fig. 7d,e,g,h). 3D GI-tomographic analysis confirmed structural integrity of the scaffold network with initial degradation of the PGA-component. No calcification or osteoid formation could be observed in GI within the explanted tissues.

Supplementary data related to this article can be found online at doi:10.1016/j.biomaterials.2011.11.087.

Biomechanical evaluation was performed separately for the valvular leaflets and the wall region. Tensile-testing of the conduit explants revealed increasing tissue strength as well as stiffness after several days in vivo when compared to the composite matrix (Fig. 7i). The Modulus of Elasticity (EM) for the conduit wall (41.47 [MPa]) was higher than the EM of the PGA-P4HB composite matrix (6.87 [MPa]). This clear difference in the stress-strain behavior suggests initial tissue formation and matrix remodeling throughout one week in situ. Nano-indentation analysis of the leaflet showed elasticity characteristics (EM; 2.7 kPA) potentially compatible with biological tissue also suggesting bio-mechanically relevant neo-tissue formation in the TEHV leaflets (Fig. 7j).

## 4. Discussion

Congenital heart valve disease affects up to 0.2% of all newborns [23]. In particular, aortic or pulmonary valve stenosis causes a substantial disease load resulting in severe midgestational myocardial damage with development of hypoplastic left/right heart syndrome. In case of fetal survival, patients are facing multiple palliative surgical procedures with a prospect of lifelong cardiac disability [13,17]. Therefore, prenatal repair of selected patients has recently become the focus of intense clinical investigation in centers worldwide mainly performing interventional ballon valvuloplasty to dilate stenotic segments [16–19]. While this repair at the earliest possible time point has been shown to improve the outcome of selected cases [16–21,24,25], re-stenosis of the obstructed segments has repeatedly been reported after prenatal cardiac balloon interventions [17,21,25]. Therefore – based on these initial encouraging results - a definite valvular repair or replacement in the fetus fully restoring valve functionality and preventing re-obstruction would represent a next generation therapy for these patients even in more complex malformations [13,26]. However, such definite valvular substitutes require adaptive capacities to the substantial dimensional changes during fetal growth and the later postnatal development. Therefore, tissue engineered autologous cell-based living heart valves with growth and remodeling capacities may represent a more ideal fetal valve substitute.

The presented study demonstrates the feasibility of the prenatal transapical implantation of autologous fetal cell-based tissue engineered heart valves in the ovine fetal model with acute and chronic survival. Importantly, the presented approach merges several recent technological innovations - that is amniotic fluid-derived stem cell technologies [27], single step heart valve tissue engineering technologies [6,28–30], minimally invasive transapical implantation techniques [4,6] and fetal cardiac intervention [13]. While the transapical implantation of tissue engineered heart valves has been previously demonstrated [4], the extensive, logistically complex, and time-consuming in-vitro tissue engineering processes have motivated the development of single step cell-based approaches [6,30]. In particular, in fetal cardiac interventions with narrow gestational windows for therapeutic intervention, a cell-based single step approach appears favorable.

The feasibility of the single-step in-situ tissue engineering approach has been demonstrated for vascular grafts and heart valves using bone marrow-derived mononuclear cells (BMCs [6,7,28–31];) and mesenchymal cells [32] in experimental as well as clinical settings. While unseeded controls rendered long-term structural failure in the ovine model [6], seeded constructs were shown to have enhanced cellular infiltration in the acute phase [28–30] followed by enhanced tissue formation [31]. In a recent study, *Roh* et al. [30] elucidated the potential underlying molecular mechanism of autologous BMC-induced tissue formation. In contrast to previous assumptions, no evidence for (trans-) differentiation of bone marrow-derived stem cells into mature vascular cells has been found. In fact, it was shown that cell-seeded biodegradable scaffolds transform into functional tissues via an inflammation-mediated process of host progenitor and immune cell attraction and subsequent remodeling involving factors like MCP-1, IL-6 and VEGF secreted by the seeded cells. Interestingly, recent investigations also revealed a similar pro-angiogenic potential for human amniotic fluid-derived cells (hAFCs) in vitro and in vivo. AFCs were shown to secrete high amounts of common pro-angiogenic/chemo-attractive factors – including MCP-1, VEGF, IL-6, IL-8, EGF and SDF-1 – and thereby significantly attracted endothelial progenitor cells in vitro [33–36]. Also this study confirms these reports by identifying several pro-angiogenic (IL-8, CXCL-1) and immunomodulatory (MIF, IL6) factors in supernatants of scaffold-seeded AFCs. In addition, it was recently demonstrated that hAFC-seeded scaffolds recruited high amounts of monocytes/macrophages, endothelial/mesenchymal progenitor cells, and bone marrow-derived cells to the implantation site when compared to unseeded scaffold controls [35,36]. Importantly, in a direct comparison the pro-angiogenic capacity of hAFCs was even found to be significantly higher than that of bone marrow-derived cells [35], which have previously shown to have a major chemo-attractive potential on various immune cells [37–39].

In accordance with these previous findings, the cellularity in TEHVs was also increased in AFC-pre-seeded constructs in the present investigation already after a few hours in-vivo (however, without correction for pre-seeded AFCs). Histology demonstrated

filaments (f/g: arrows indicate neo-tissue formation). Although partial degradation of scaffold matrix is detectable, the composite scaffold matrix is still present in the explanted constructs (f–g). The degradation zones were mainly located close to the surface of the explanted tissues with a cluster-like distribution of the degradation and a central almost non-degraded matrix block. Uniaxial tensile testing allows for a direct comparison of the stress-strain behavior of 1 week explants and PGA-P4HB composite matrices demonstrating a clear difference in mechanical properties (i). Nano-indentation testing of the TEHV leaflet (BRGA explant) rendered a force-penetration curve that is divided into a loading (blue) and unloading (red) phase with a Modulus of Elasticity of $E = 2.7$ kPa (j). (For interpretation of the references to colour in this figure legend, the reader is referred to the web version of this article.)

high cellularity with profound phagocytic accumulation in pre-seeded midterm explants as well as a distinct macrophage infiltration in chronic BRGA explants. This also suggests a cell-attractive potential of seeded ovine AFCs similar to the investigations reported above for non-cardiovascular implants. Interestingly, also in the present study this process was paralleled by a substantial decrease of the initially seeded AFCs as also demonstrated for bone marrow cell-based cardiovascular implants [30] and non-cardiovascular AFC-seeded implants [35,36].

*Shaw* et al. [40] first investigated the fate of autologous amniotic fluid-derived mesenchymal stem cells prenatally in the ovine fetal model. After harvesting, GFP-labeling and in vitro expansion, cells were re-injected into the peritoneal cavity of mid-gestation fetuses. At birth, analysis revealed widespread organ migration of cells, suggesting participation in growth and remodeling processes. Furthermore, *Klein* et al. [41] identified autologous AFCs as exogenous cellular components in naturally occurring healing processes of the skin. Within these defects AFCs were shown to expedite wound closure and enhance the extracellular matrix profile. These properties of AFCs with their contribution to regenerative processes may have been advantageous with regard to AFC-seeded valvular tissue engineered constructs in the current study, as the TEHVs primarily represent areas of intense healing and remodeling. Given the fetal scarless healing reactions [10] and the enhanced fetal regenerative capacity with high levels of circulating progenitor cells [12], combined with the low pressure 'bypass'-flow of the fetal circulation mimicking bioreactor-like conditions, the fetus may represent the ideal patient for a cell-based in-situ tissue engineering approach.

In the light of the poor prognosis in several congenital defects, these favorable fetal healing capacities have stipulated a major interest in broadening the spectrum of fetal cardiac interventions. While the use of fetal cardiac bypass appeared to be complex [42], several experimental studies explored alternative minimally invasive routes to the fetal heart. This involved transuterine fetoscopic [14], transhepatic [15], or transumbilical [14] routes. Although encouraging, acute perioperative complications, such as major bleeding or bradycardia, have been reported and long-term survival in catheter-based percutaneous or transuterine procedures varied between 42 and 50% [14,15]. Also in the present investigation, substantial mortality occurred, certainly representing a major limitation of the study. While the surgical deployment was successful in all experimental cases, the acute survival after deployment mainly correlated with the perioperative blood loss at the antero-apical insertion site. Given the prototypic design of the delivery device with a diameter of 14 French, acute fetal loss at implantation may be minimized and survival until birth improved by a more advanced delivery system in the future.

## 5. Conclusions

In summary, we demonstrate the feasibility of the prenatal in-vitro fabrication and fetal transapical implantation of amniotic fluid stem cell-based heart valves in the ovine fetal model with acute and chronic survival until birth. This autologous cell-based in-situ tissue engineering approach may serve as a basis for future human prenatal heart valve repair using autologous living fully biodegradable substitutes. Future studies will have to further investigate the role of seeded autologous fetal cells as well as the long-term performance of prenatally delivered valvular constructs.

## Conflict of interest statement

S.P.H. and G.Z. are scientific advisors of Xeltis AG, Switzerland. Luc B. is an employee of IMMR, Paris.

## Acknowledgements

The current study represents a collaborative approach. The authors thank Sébastien Sammut (IMMR), Mehrak Hekmati (IMMR), Stephan Weiss (Scanco Medical Inc.), Klaus Marquardt (ZMBZ), Silivia Behnke, Jan Klohs, Michele Sidler, Ulrich Bleul, Josef Achermann, Guido Savoldelli, Pia Fuchs, Réne Stenger, Simone Bolliger (Cook Medical Inc.), Francesca Papadopulos, Ursula Steckholzer, Petra Wolint, Mårten Schneider and Burkhardt Seifert (IFSPM). This work was supported by the Swiss Government [EX25-2010]; the Swiss National Science Foundation [IZK0Z3], [32-122273] and [124090]; the 7th Framework Programme, Life Valve, European Commission [242008], the Marco-Polo Fellowship, the Centre d'Imagerie BioMedicale (CIBM) of the UNIL, UNIGE, HUG, CHUV, EPFL, the Leenaards and the Jeantet Foundations.

## Appendix. Supplementary data

Supplementary data related to this article can be found online at doi:10.1016/j.biomaterials.2011.11.087.

## References

[1] Schoen FJ. Evolving concepts of cardiac valve dynamics: the continuum of development, functional structure, pathobiology, and tissue engineering. Circulation 2008;118:1864–80.
[2] Schmidt D, Mol A, Breymann C, Achermann J, Odermatt B, Goessi M, et al. Living autologous heart valves engineered from human prenatally harvested progenitors. Circulation 2006;114:I125–31.
[3] Schmidt D, Achermann J, Odermatt B, Breymann C, Mol A, Genoni M, et al. Prenatally fabricated autologous human living heart valves based on amniotic fluid derived progenitor cells as single cell source. Circulation 2007;116:I64–70.
[4] Schmidt D, Dijkman PE, Driessen-Mol A, Stenger R, Mariani C, Puolakka A, et al. Minimally-invasive implantation of living tissue engineered heart valves: a comprehensive approach from autologous vascular cells to stem cells. J Am Coll Cardiol 2010;56:510–20.
[5] Dahl SL, Kypson AP, Lawson JH, Blum JL, Strader JT, Li Y, et al. Readily available tissue-engineered vascular grafts. Sci Transl Med 2011;68:68–9.
[6] Weber B, Scherman J, Emmert MY, Gruenenfelder J, Verbeek R, Bracher M, et al. Injectable living marrow stromal cell-based autologous tissue engineered heart valves: first experiences with a one-step intervention in primates. Eur Heart 2011;32:2830–40.
[7] Emmert MY, Weber B, Behr L, Frauenfelder T, Brokopp C, Grunenfelder J, et al. Aortic Implantation of marrow stromal cell-based tissue engineered heart valves – first experiences in the systemic circulation. JACC Cardiovasc Interv 2011;4:822–3.
[8] Mujezinovic F, Alfirevic Z. Procedure-related complications of amniocentesis and chorionic villous sampling: a systematic review. Obstet Gynecol 2007;110:687–94.
[9] Weber B, Zeisberger SM, Hoerstrup SP. Prenatally harvested cells for cardiovascular tissue engineering: fabrication of autologous iImplants prior to birth. Placenta 2011;32:316–9.
[10] Coolen NA, Schouten KC, Boekema BK, Middelkoop E, Ulrich MM. Wound healing in a fetal, adult, and scar tissue model: a comparative study. Wound Repair Regen 2010;18:291–301.
[11] Gurtner GC, Werner S, Barrandon Y, Longaker MT. Wound repair and regeneration. Nature 2008;453:314–21.
[12] Iwasaki H, Kawamoto A, Willwerth C, Horii M, Oyamada A, Akimaru H, et al. Therapeutic potential of unrestricted somatic stem cells isolated from placental cord blood for cardiac repair post myocardial infarction. Arterioscler Thromb Vasc Biol 2009;29:1830–5.
[13] McElhinney DB, Tworetzky W, Lock JE. Current status of fetal cardiac intervention. Circulation 2010;121:1256–63.
[14] Kohl T, Szabo Z, Suda K, Petrossian E, Ko E, Kececioglu D, et al. Fetoscopic and open transumbilical fetal cardiac catheterization in sheep: potential approaches for human fetal cardiac intervention. Circulation 1997;95:1048–53.
[15] Jouannic JM, Boudjemline Y, Benifla JL, Bonnet D. Transhepatic ultrasound-guided cardiac catheterization in the fetal lamb: a new approach for cardiac interventions in fetuses. Circulation 2005;111:736–41.
[16] Tulzer G, Arzt W, Franklin RC, Loughna PV, Mair R, Gardiner HM. Fetal pulmonary valvuloplasty for critical pulmonary stenosis or atresia with intact septum. Lancet 2002;360:1567–8.
[17] Tworetzky W, Wilkins-Haug L, Jennings RW, van der Velde ME, Marshall AC, Marx GR, et al. Balloon dilation of severe aortic stenosis in the fetus: potential for prevention of hypoplastic left heart syndrome: candidate selection,

technique, and results of successful intervention. Circulation 2004;110: 2125–31.
[18] McElhinney DB, Marshall AC, Wilkins-Haug LE, Brown DW, Benson CB, Silva V, et al. Predictors of technical success and postnatal biventricular outcome after in utero aortic valvuloplasty for aortic stenosis with evolving hypoplastic left heart syndrome. Circulation 2009;120:1482–90.
[19] Kohl T, Tchatcheva K, Van de Vondel P, Gembruch U. Intraamniotic fetal echocardiography: a new fetal cardiovascular monitoring approach during human fetoscopic surgery. Circulation 2006;114:594–6.
[20] Galindo A, Gutiérrez-Larraya F, Velasco JM, de la Fuente P. Pulmonary balloon valvuloplasty in a fetus with critical pulmonary stenosis/atresia with intact ventricular septum and heart failure. Fetal Diagn Ther 2006;21:100–4.
[21] Wilkins-Haug LE, Tworetzky W, Benson CB, Marshall AC, Jennings RW, Lock JE. Factors affecting technical success of fetal aortic valve dilation. Ultrasound Obstet Gynecol 2006;28:47–52.
[22] Mol A, van Lieshout MI, Dam-de Veen CG, Neuenschwander S, Hoerstrup SP, Baaijens FP, et al. Fibrin as a cell carrier in cardiovascular tissue engineering applications. Biomaterials 2005;26:3113–21.
[23] Hoffman JI, Kaplan S. The incidence of congenital heart disease. J Am Coll Cardiol 2002;39:1890–900.
[24] Kohl T, Sharland G, Allan LD, Gembruch U, Chaoui R, Lopes LM, et al. World experience of percutaneous ultrasound-guided balloon valvuloplasty in human fetuses with severe aortic valve obstruction. Am J Cardiol 2000;85: 1230–3.
[25] Selamet Tierney ES, Wald RM, McElhinney DB, Marshall AC, Benson CB, Colan SD, et al. Changes in left heart hemodynamics after technically successful in-utero aortic valvuloplasty. Ultrasound Obstet Gynecol 2007;30: 715–20.
[26] Weber B, Emmert MY, Behr L, Brokopp C, Frauenfelder T, Kretschmar O, et al. Fetal trans-apical stent delivery into the pulmonary artery: prospects for prenatal heart valve implantation. Eur J Cardiothor Surg; 2011:7.
[27] De Coppi P, Bartsch Jr G, Siddiqui MM, Xu T, Santos CC, Perin L, et al. Isolation of amniotic stem cell lines with potential for therapy. Nat Biotechnol 2007;25:100–6.
[28] Shin'oka T, Imai Y, Ikada Y. Transplantation of a tissue-engineered pulmonary artery. N Engl J Med 2001;344:532–3.
[29] Brennan MP, Dardik A, Hibino N, Roh JD, Nelson GN, Papademitris X, et al. Tissue-engineered vascular grafts demonstrate evidence of growth and development when implanted in a juvenile animal model. Ann Surg 2008; 248:370–7.
[30] Roh JD, Sawh-Martinez R, Brennan MP, Jay SM, Devine L, Rao DA, et al. Tissue-engineered vascular grafts transform into mature blood vessels via an inflammation-mediated process of vascular remodeling. Proc Natl Acad Sci U S A 2010;107:4669–728.
[31] Mirensky TL, Hibino N, Sawh-Martinez RF, Yi T, Villalona G, Shinoka T, et al. Tissue-engineered vascular grafts: does cell seeding matter? J Pediatr Surg 2010;45:1299–305.
[32] Jux C, Bertram H, Wohlsein P, Brügmann M, Wüboldt P, Fink C, et al. Experimental ASD closure using autologous cell-seeded interventional closure devices. Cardiovasc Res 2002;53:181–91.
[33] Yoon BS, Moon JH, Jun EK, Kim J, Maeng I, Kim JS, et al. Secretory profiles and wound healing effects of human amniotic fluid-derived mesenchymal stem cells. Stem Cells Dev 2010;19(6):887–902.
[34] Perin L, Sedrakyan S, Giuliani S, Da Sacco S, Carraro G, Shiri L, et al. Protective effect of human amniotic fluid stem cells in an immunodeficient mouse model of acute tubular necrosis. PLoS One 2010;24:9357.
[35] Teodelinda M, Michele C, Sebastiano C, Ranieri C, Chiara G. Amniotic liquid derived stem cells as reservoir of secreted angiogenic factors capable of stimulating neo-arteriogenesis in an ischemic model. Biomaterials 2011;32: 3689–99.
[36] Mirebella T, Poggi A, Scaranari M, Mogni M, Lituania M, Baldo C, et al. Recruitment of host's progenitor cells to sites of human amniotic fluid stem cells implantation. Biomaterials 2011;32:4218–27.
[37] Brandau S, Jakob M, Hemeda H, Bruderek K, Janeschik S, Bootz F, et al. Tissue-resident mesenchymal stem cells attract peripheral blood neutrophils and enhance their inflammatory activity in response to microbial challenge. J Leukoc Biol 2010;88:1005–15.
[38] Sumanasinghe RD, Pfeiler TW, Monteiro-Riviere NA, Loboa EG. Expression of proinflammatory cytokines by human mesenchymal stem cells in response to cyclic tensile strain. J Cell Physiol 2009;219:77–83.
[39] Romieu-Mourez R, François M, Boivin MN, Bouchentouf M, Spaner DE, Galipeau J. Cytokine modulation of TLR expression and activation in mesenchymal stromal cells leads to a proinflammatory phenotype. J Immunol 2009; 182:7963–73.
[40] Shaw SS, Bollini S, Abi Nader K, Gastadello A, Mehta V, Filppi E, et al. Autologous transplantation of amniotic fluid derived mesenchymal stem cells into sheep fetuses. Cell Transplant 2011;20:1015–31.
[41] Klein JD, Turner CG, Steigman SA, Ahmed A, Zurakowski D, Eriksson E, et al. Amniotic mesenchymal stem cells enhance normal fetal wound healing. Stem Cells Dev 2010;20:969–76.
[42] Ikai A, Riemer RK, Ramamoorthy C, Malhotra S, Cassorla L, Amir G, et al. Preliminary results of fetal cardiac bypass in nonhuman primates. J Thorac Cardiovasc Surg 2005;129:175–81.